

Predicting Soil Hydraulic Properties from Particle Size Distribution and X-Ray Tomography.



Yann Periard (1), Silvio José Gumiere (1), Alain N. Rousseau (2), Dennis W. Hallema (1), and Jean Caron (1)

yann.periard-larrivee.1@ulaval.ca

(1) Université Laval, Faculté des sciences de l'agriculture et de l'alimentation, Département des sols et de génie agroalimentaire, Québec, Canada ,

(2) Institut national de la recherche scientifique : Centre Eau Terre Environnement (INRS-ETE), Québec, Canada, QC



Session: Revisiting the Most Important Curve in Soil Physics: II

Poster Number 1401

Introduction

- Knowledge about soil hydraulic properties are fundamental
- Characterization of these properties is very time-consuming
- Requires many sample manipulations
- Advances in the field of tomography imagery allow for the characterization of a number of soil hydraulic properties (Wildenschild and Sheppard, 2013)
- The use of the μ CT-scan is limited to very small sample (<10 cm³), which is inappropriate to study a representative volume of soil (soil profiles).

Objective

- The main objective of this work is to propose a framework to predict soil hydraulic properties from the combination of particle size distribution with X-ray tomography of a porous media.

Materials & Methods

1. Soils characterization

- Soil sample contained in a 15-cm long, 5-cm wide cylinder
- Unconsolidated Ottawa sand
- Curves of water retention and hydraulic conductivity obtained using the instantaneous profile method

2. Particle distribution

- Particle size distribution = LA950v2 Laser Particle Size Analyzer (Horiba)
- n th moment

$$m_n = \exp\left(n\mu_y + \frac{n^2\sigma_y^2}{2}\right)$$

Cumulative mass fraction

$$M(R) = W \left(1 - \frac{1}{2} \operatorname{erfc}\left(\frac{\ln R - (\mu_y + 3\sigma_y^2)}{\sqrt{2}\sigma_y}\right)\right) + (1-W) \left(1 - \frac{1}{2} \operatorname{erfc}\left(\frac{\ln R - (\mu_y + 3\sigma_y^2)}{\sqrt{2}\sigma_y}\right)\right)$$

μ_y = mean of $\ln R$
 σ_y = standard deviation of $\ln R$
 W = weighting factor for the i th sub-distribution

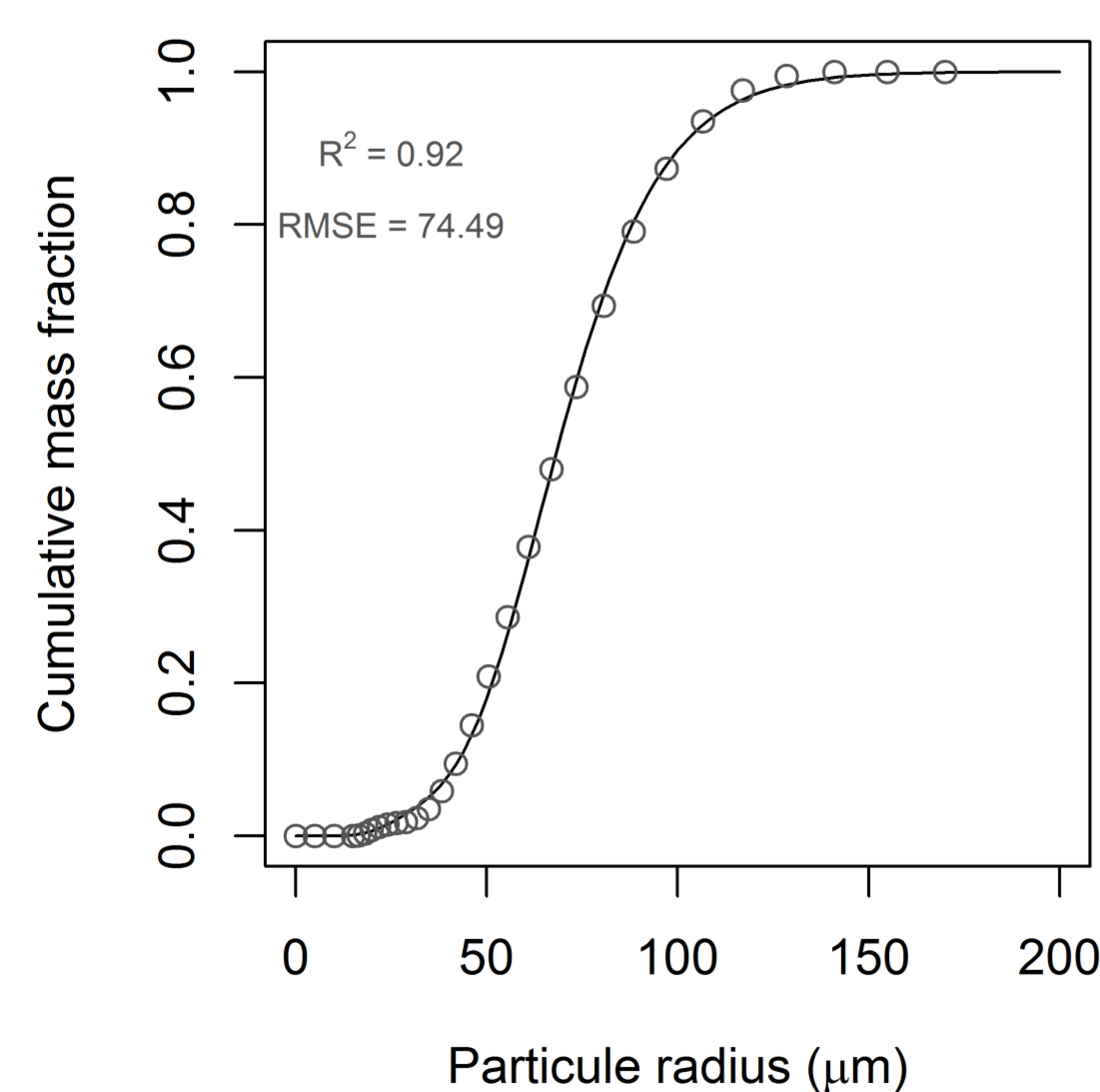


Figure 1. Cumulative mass fraction of particle sizes (R)

Materials & methods

3. Derivation of soil hydraulic properties

- Carnahan–Starling approximation of void nearest-surface complementary cumulative density function (Chan and Govindaraju, 2004)

$$e_{vn}(\delta) = (1-\eta) \exp\left\{-\eta S \left[a_0 \left(\frac{\delta}{m_1}\right)^3 + a_1 \left(\frac{\delta}{m_1}\right)^2 + a_2 \left(\frac{\delta}{m_1}\right) \right]\right\} \text{ where } S = \frac{m_1 m_2}{m_3} \quad \eta = 1 - \phi$$

$$a_0 = \frac{(m_1^2/m_2)(1-\eta)(1-\eta+3\eta S) + 2\eta^2 S^2}{(1-\eta)^3}$$

$$a_1 = \frac{6(m_1^2/m_2)(1-\eta) + 9\eta S}{2(1-\eta)^2} \quad a_2 = \frac{3}{1-\eta}$$

- Coefficients a_0, a_1, a_2
- S = surface ratio
- η = dimensionless reduced density

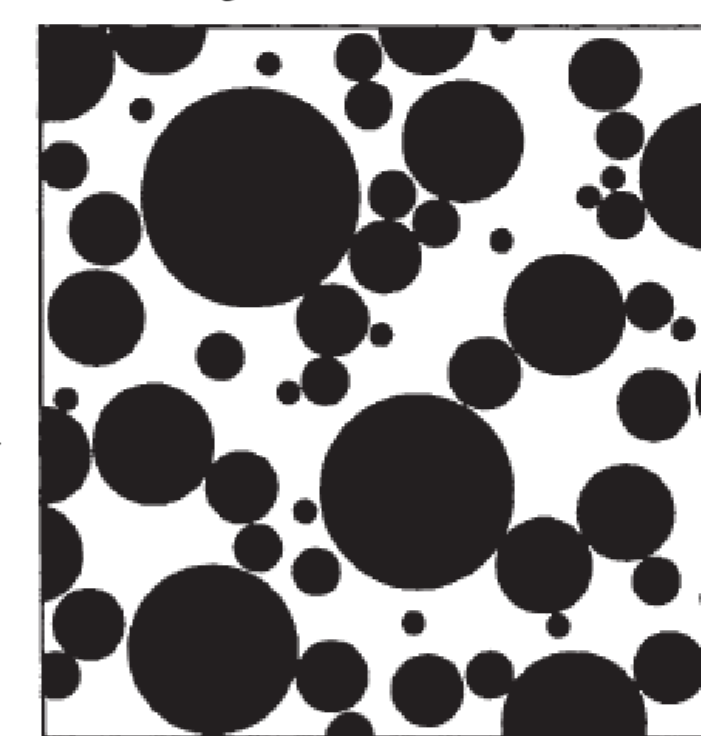


Figure 2. Polydisperse impenetrable hard spheres systems in 2D (Chan and Govindaraju, 2004)

- Nearest solid surface

$$\delta = ae^{br} \quad r = \frac{2\sigma \cos \Psi}{\rho gh}$$

- Coefficients a, b
- σ = interfacial tension
- Ψ = contact angle
- g = gravitational acceleration
- ρ = density of the fluid
- h = soil matric potential

- Effective saturation

$$S_e = W \left(1 - \frac{e_{v1}}{\phi}\right) + (1-W) \left(1 - \frac{e_{v2}}{\phi}\right)$$

- Relative hydraulic conductivity (Mualem, 1976)

$$Kr = S_e^\tau \left[W \left(\frac{\int_0^{S_{e1}} \frac{1}{\psi(S_{e1})} dS_{e1}}{\int_0^W \frac{1}{\psi(S_{e1})} dS_{e1}} \right) + (1-W) \left(\frac{\int_0^{S_{e2}} \frac{1}{\psi(S_{e2})} dS_{e2}}{\int_0^{1-W} \frac{1}{\psi(S_{e2})} dS_{e2}} \right) \right]$$

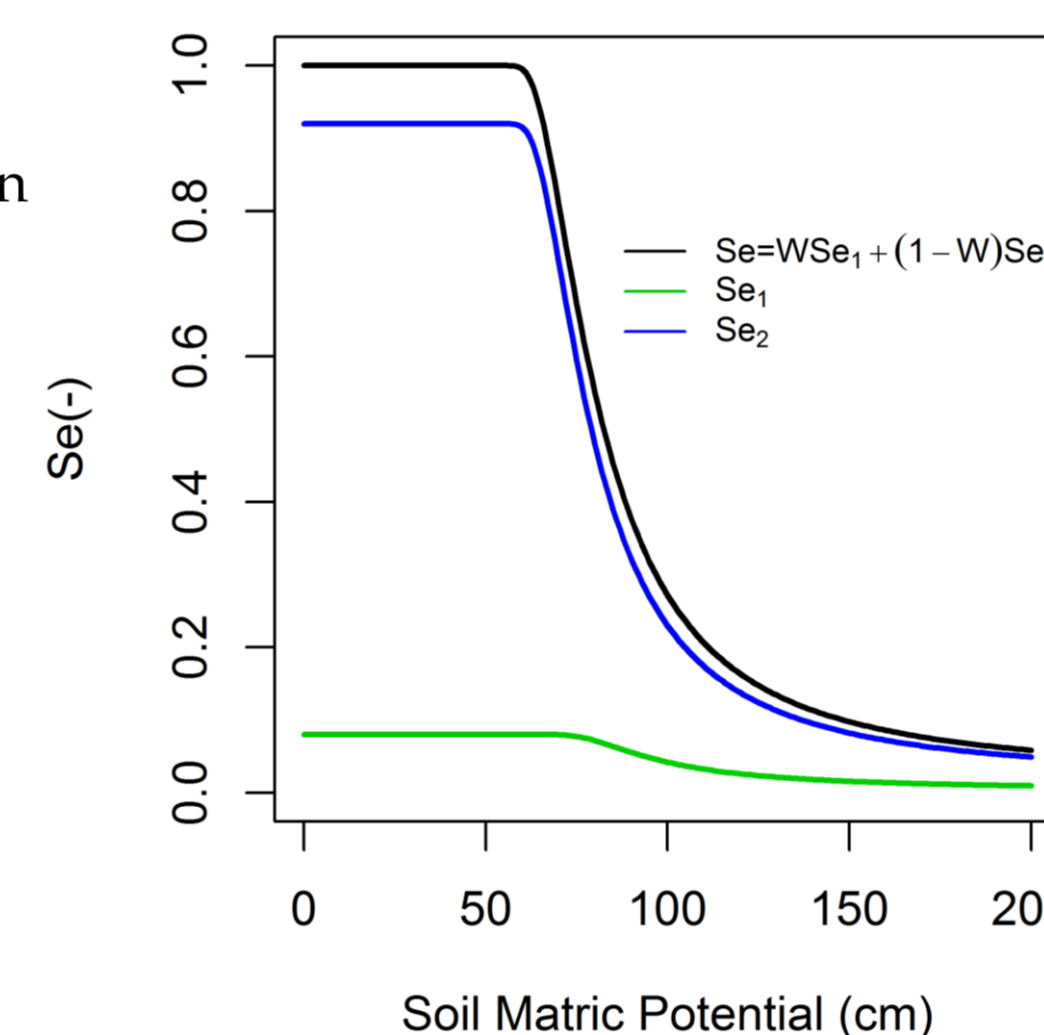


Figure 3. Dual model of effective saturation

4. Tomographic analysis

- The study was done at *Laboratoire Multidisciplinaire de Scanographie du Québec de l'INRS-ETE*.
- Type of Medical CT scan : Somatom Volume Access (Siemens, Oakville, ON, CA).
- Energy level of 140, 120, 100 and 80 keV
- Voxel resolution of 0.1x0.1x0.6 mm



Figure 4. Medical CT scan

Determination of the porosity

Beer-Lambert law

$$I = I_0 \exp(-\mu x) \quad HU = 1000(\mu - \mu_w) / (\mu_w - \mu_a)$$

HU = attenuation coefficient of the soil
 HU_{quartz} = attenuation coefficient of quartz
 HU_{air} = attenuation coefficient of air

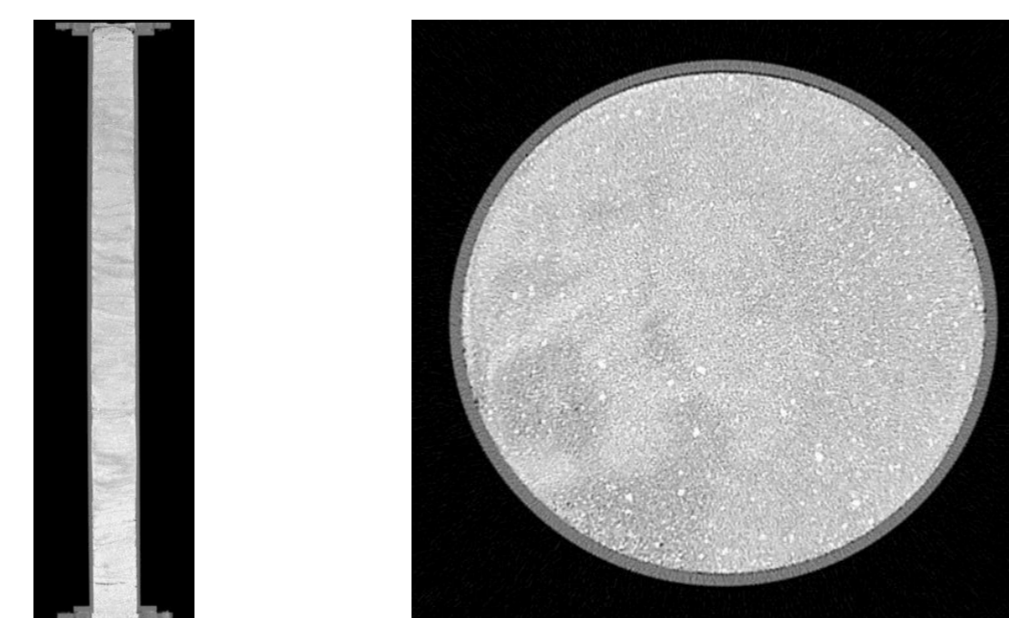


Figure 5. Vertical and horizontal slices

Conclusion

- Used and analysis of Medical CT scans clearly show the variability of soil hydraulic properties in the sample.
- The framework provides a good prediction of the mean soil hydraulic properties.
- The framework provides an opportunity to study the variability of soil hydraulic properties over a monolith.

References

- Chan, T.P., and R.S. Govindaraju. 2004. Estimating soil water retention curve from particle-size distribution data based on polydisperse sphere systems. *Vadose Zone J.* 3:1443–1454.
- Wildenschild, D. and A.P. Sheppard. 2013. X-ray imaging and analysis techniques for quantifying pore-scale structure and processes in subsurface porous medium systems. *Advances in Water Resources* 51: 217-246. doi:http://dx.doi.org/10.1016/j.advwatres.2012.07.018.

Results

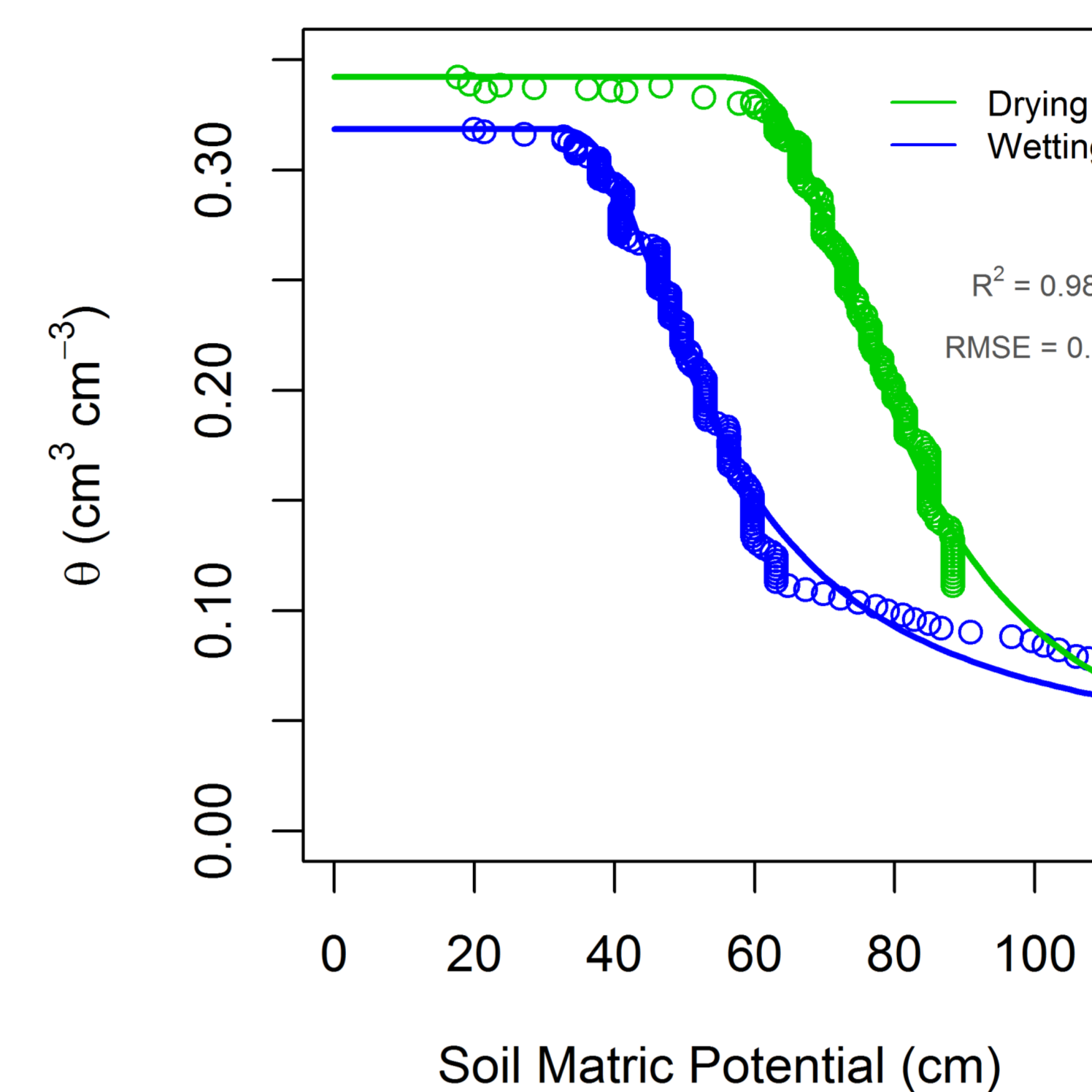


Figure 6. Soil water retention curves

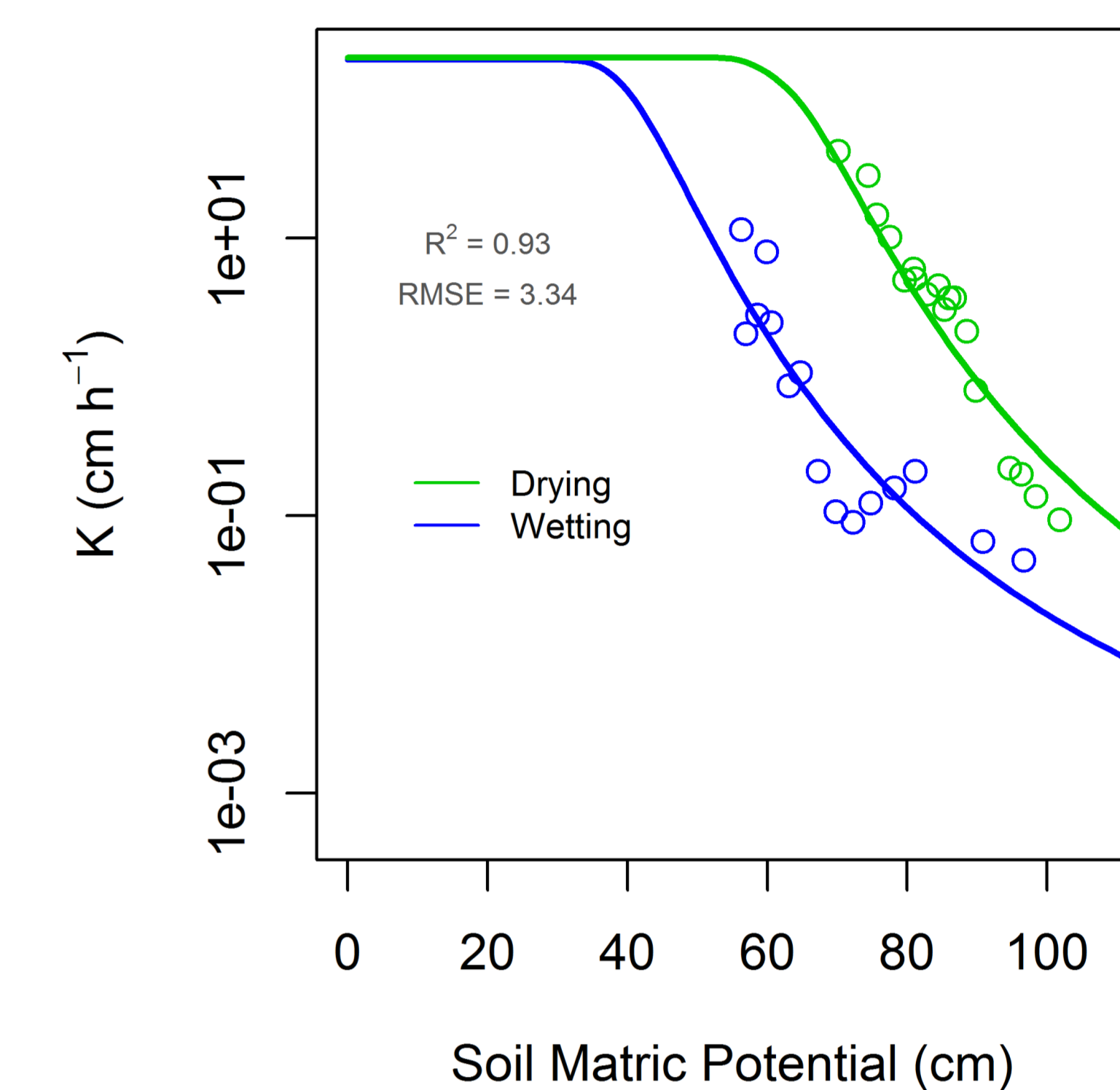


Figure 7. Soil hydraulic conductivity curves

- Good performance of the models to predict soil hydraulic properties (Figures 6 & 7)

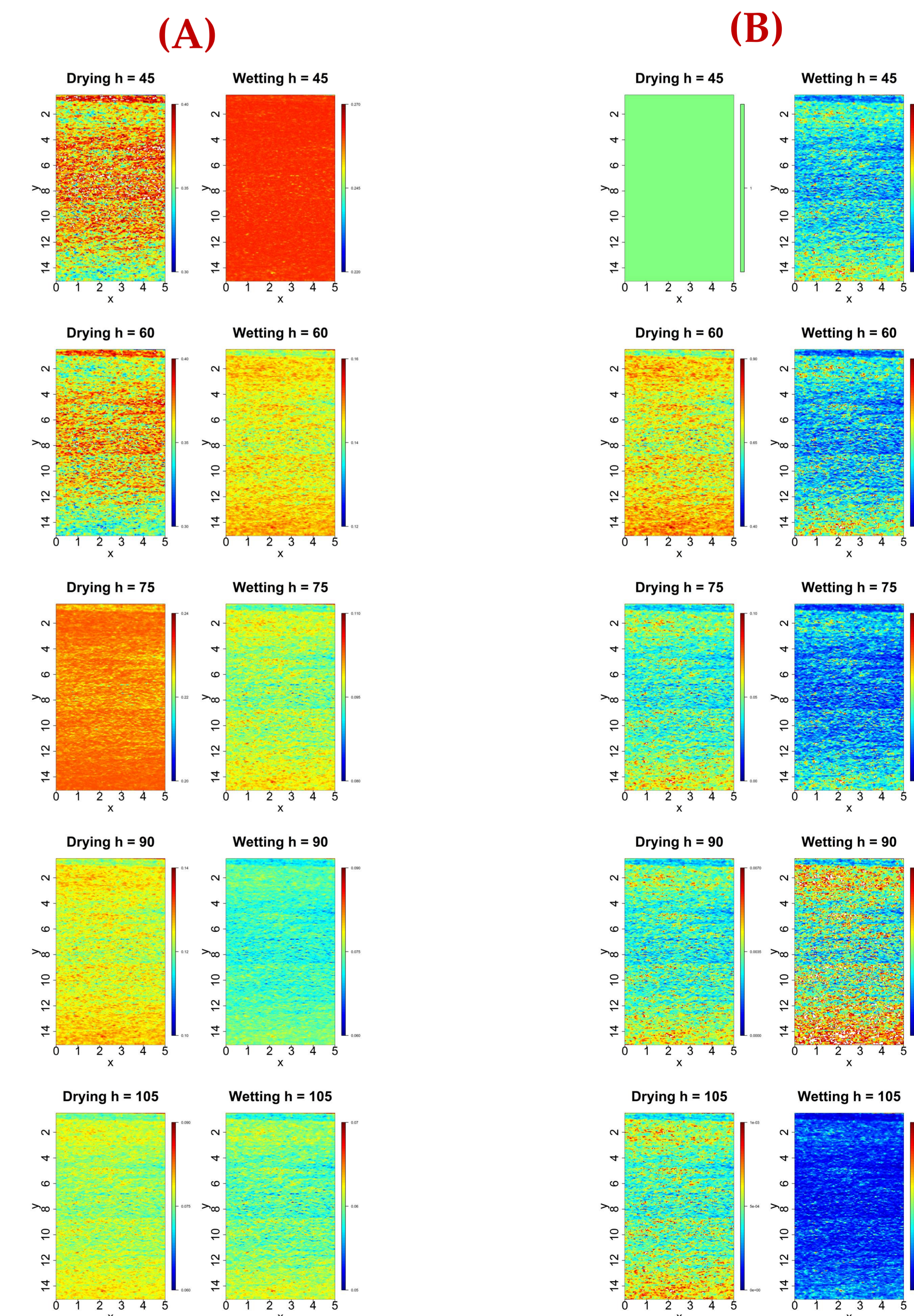


Figure 8. Radial plane of soil water content (A) and relative hydraulic conductivity (B) as a function of soil matric potential (h).

- High variability of soil hydraulic properties (Figure 8)
- Specifically in position of the curve with high variation of water content and relative hydraulic conductivity according to the matric potential (h).

Acknowledgements

